

Superconducting/ferromagnetic diffusive bilayer with a spin-active interface: A numerical study

Audrey Cottet^{1,2} and Jacob Linder³

¹*Ecole Normale Supérieure, Laboratoire Pierre Aigrain, 24 rue Lhomond, 75005 Paris, France*

²*CNRS UMR8551, Laboratoire associé aux universités Pierre et Marie Curie et Denis Diderot, France*

³*Department of Physics, Norwegian University of Science and Technology, N-7491 Trondheim, Norway*
(Received 2 October 2008; revised manuscript received 3 December 2008; published 17 February 2009)

We calculate the density of states (DOS) in a diffusive superconducting/ferromagnetic bilayer with a spin-active interface. We use a self-consistent numerical treatment to make a systematic study of the effects of the spin dependence of interfacial phase shifts (SDIPS) on the self-consistent superconducting gap and the DOS. Strikingly, we find that the SDIPS can induce a double gap structure in the DOS of the ferromagnet, even when the superconducting layer is much thicker than the superconducting coherence length. We thus obtain DOS curves which have interesting similarities with those of SanGiorgio *et al.* [Phys. Rev. Lett. **100**, 237002 (2008)].

DOI: [10.1103/PhysRevB.79.054518](https://doi.org/10.1103/PhysRevB.79.054518)

PACS number(s): 73.23.-b, 74.20.-z, 74.50.+r

I. INTRODUCTION

Superconducting/ferromagnetic (S/F) hybrid structures give rise to a fascinating interplay between two antagonist electronic orders. The ferromagnetic exchange field E_{ex} privileges one spin direction while standard superconductivity favors singlet correlations. This leads to a rich behavior which has triggered an intense activity in the last years (see, e.g., Refs. 1 and 2). In particular, the “superconducting proximity effect,” i.e., the propagation of the superconducting correlations in ferromagnets, has been widely studied. This propagation is accompanied by spatial oscillations of the superconducting order parameter because E_{ex} induces an energy shift between electrons and holes. As a result, one can build electronic devices with new functionalities, such as Josephson junctions with negative critical currents,³ which could find applications in the field of superconducting circuits.^{4,5} From a fundamental point of view, it is very instructive to study the density of states (DOS) of S/F structures. So far, this quantity has been less measured^{6–10} than critical temperatures or supercurrents. However, this way of probing the superconducting proximity effect is very interesting because it provides spectroscopic information. One striking consequence of the spatial oscillations of the order parameter in the F layer is that the zero-energy DOS can become larger than in the normal state for certain ferromagnet thicknesses.⁶

The behavior of S/F hybrid circuits depends crucially on the properties of the interfaces between the S and F materials. In this paper, we focus on the case of diffusive structures. Diffusive S/F interfaces have been initially described with spin-independent boundary conditions.¹¹ It has been found that the amplitude of the superconducting proximity effect directly depends on the tunnel conductance G_T of an interface (see, e.g., Ref. 1). Later, spin-dependent boundary conditions have been introduced in the limit of a weakly polarized ferromagnet.^{12,13} Due to the spin dependence of interfacial phase shifts (SDIPS),^{14–16} one has to take into account new conductance parameters G_ϕ^F and G_ϕ^S at the F and S sides of the interface, respectively. It has been shown that G_ϕ^F and G_ϕ^S can significantly affect the behavior of S/F hybrid

circuits. For instance, G_ϕ^F can shift the spatial oscillations of the superconducting order parameter.¹³ More recently, it has been found that G_ϕ^S can induce an effective Zeeman splitting Δ_Z^{eff} in a superconducting layer with a thickness d_S smaller than the superconducting coherence length scale ξ_S .¹⁷ This induces a double gap structure (DGS) in the S and F densities of states. However, in practice, the regime $d_S \geq \xi_S$ is frequently reached (see, e.g., Refs. 18 and 19). Remarkably, DGSs have been recently observed at the F side of Ni/Nb bilayers with d_S much larger than ξ_S ,¹⁰ although Ref. 17 has found that Δ_Z^{eff} scales with d_S^{-1} in the low- d_S regime. Whether a DGS persists in the large- d_S regime is therefore an important question, especially in the light of this recent experiment.

In this paper, we study how G_ϕ^F and G_ϕ^S modify the DOS of a S/F bilayer. We use a numerical treatment to explore a wider parameter range than in previous works. In particular, we can reach the limit of thick superconductors and larger values of G_ϕ^S . We find that G_ϕ^S shifts the spatial oscillations of the superconducting order parameter in F , similarly to G_ϕ^F . It can also significantly affect the amplitude of the superconducting gap. When d_S increases, the SDIPS-induced DGS becomes narrower, in agreement with Ref. 17. Nevertheless, it can surprisingly persist in the large- d_S limit. Indeed, in a distance of the order of ξ_S near the S/F interface, the resonance energies of the S spectrum remain spin dependent because quantum interferences make the superconducting correlations sensitive to the SDIPS. This behavior is transmitted to the whole F layer due to the superconducting proximity effect. We thus obtain, at the F side of S/F bilayers, DOS curves which have interesting similarities with those of Ref. 10, although $d_S \gg \xi_S$. More generally, our results could be useful for interpreting experiments.

This paper is organized as follows. Section II defines the S/F bilayer problem studied in this paper. Section III explains the principle of our numerical treatment. Section IV presents a detailed study of the SDIPS-induced DGS. Section V shows the effects of the SDIPS on the self-consistent superconducting gap and on the oscillations of the zero-energy DOS with the thickness of F . Section VI discusses the data of Ref. 10. Section VII concludes.

II. DESCRIPTION OF THE S/F BILAYER

We consider a diffusive S/F bilayer consisting of a standard BCS superconductor S for $-d_S < x < 0$ and a ferromagnet F for $0 < x < d_F$. We characterize the normal quasiparticle excitations and the superconducting condensate of pairs with the Usadel normal and anomalous Green's functions $G_{n,\sigma} = \text{sgn}(\omega_n) \cos(\theta_{n,\sigma})$ and $F_{n,\sigma} = \sin(\theta_{n,\sigma})$, with $\theta_{n,\sigma}(x)$ as the superconducting pairing angle, which depends on the spin direction $\sigma \in \{\uparrow, \downarrow\}$, $\omega_n(T) = (2n+1)\pi k_B T$ as the Matsubara frequency, and x as the spatial coordinate.²⁰ The Usadel equations describing the spatial evolution of $\theta_{n,\sigma}$ write

$$\xi_S^2 \frac{\partial^2 \theta_{n,\sigma}}{\partial x^2} = \frac{|\omega_n|}{\Delta_0} \sin(\theta_{n,\sigma}) - \frac{\Delta(x)}{\Delta_0} \cos(\theta_{n,\sigma}) \quad (1)$$

in S and

$$\xi_F^2 \frac{\partial^2 \theta_{n,\sigma}}{\partial x^2} = k_{n,\sigma}^2 \sin(\theta_{n,\sigma}) \quad (2)$$

in F with

$$k_{n,\sigma} = \sqrt{2[i\sigma \text{sgn}(\omega_n) + (|\omega_n|/E_{\text{ex}})]}. \quad (3)$$

In the above equations, Δ_0 denotes the bulk gap of the S material, $\xi_S = (\hbar D_S / 2\Delta_{\text{BCS}})^{1/2}$ is the superconducting coherence length scale, $\xi_F = (\hbar D_F / E_{\text{ex}})^{1/2}$ is the magnetic coherence length scale, $D_{F(S)}$ is the diffusion constant in $F(S)$, and E_{ex} is the ferromagnetic exchange field of F . The self-consistent superconducting gap $\Delta(x)$ occurring in Eq. (1) can be expressed as

$$\Delta(x) \log \left[\frac{T}{T_c^0} \right] = \frac{\pi k_B T}{2} \sum_{\substack{\sigma \in \{\uparrow, \downarrow\} \\ |\omega_n| \leq \Omega_D}} \left[\sin(\theta_{n,\sigma}) - \frac{\Delta(x)}{|\omega_n|} \right] \quad (4)$$

with Ω_D as the Debye frequency of S , $T_c^0 = \Delta_0 \exp(\mathcal{E}) / \pi k_B$ as the bulk transition temperature of S , k_B as the Boltzmann constant, T as the temperature, and \mathcal{E} as the Euler constant. The above equations must be supplemented with a description of the boundaries of S and F . We use $\partial \theta_{n,\sigma} / \partial x|_{x=-d_S^+} = \partial \theta_{n,\sigma} / \partial x|_{x=d_F^-} = 0$ for the external sides of the bilayer. For the S/F interface, we use the spin-dependent boundary conditions^{12,17}

$$\xi_F \frac{\partial \theta_{n,\sigma}}{\partial x} \Big|_{x=0^+} = \gamma_T \sin[\theta_{n,\sigma}^F - \theta_{n,\sigma}^S] + i \gamma_\phi^F \sigma \text{sgn}(\omega_n) \sin[\theta_{n,\sigma}^F] \quad (5)$$

and

$$\xi_S \frac{\partial \theta_{n,\sigma}}{\partial x} \Big|_{x=0^-} = \gamma \gamma_T \sin[\theta_{n,\sigma}^F - \theta_{n,\sigma}^S] - i \gamma_\phi^S \sigma \text{sgn}(\omega_n) \sin[\theta_{n,\sigma}^S] \quad (6)$$

with $\theta_{n,\sigma}^F = \theta_{n,\sigma}(x=0^+)$ and $\theta_{n,\sigma}^S = \theta_{n,\sigma}(x=0^-)$. These equations involve the reduced conductances $\gamma_T = G_T \xi_F / A \sigma_F$ and $\gamma_\phi^{F(S)} = G_\phi^{F(S)} \xi_{F(S)} / A \sigma_{F(S)}$, the barrier asymmetry coefficient $\gamma = \xi_S \sigma_F / \xi_F \sigma_S$, the normal-state conductivity $\sigma_{F(S)}$ of the $F(S)$ material, and the junction area A . Note that we have used a definition of γ_ϕ^S which differs from that of Ref. 17 to ensure

a symmetric treatment of γ_ϕ^F and γ_ϕ^S in Eqs. (5) and (6). The term G_T corresponds to the usual tunnel conductance of the interface. Like G_T , the terms G_ϕ^F and G_ϕ^S can be defined microscopically from the scattering parameters of the S/F interface (see definitions in Ref. 17). The terms G_ϕ^F and G_ϕ^S can be finite only in case of a SDIPS. The SDIPS results from the fact that the scattering phases picked up by electrons upon scattering by the S/F interface can depend on spin due to the ferromagnetic exchange field or to a spin-dependent interface potential. Thus, in principle, any kind of S/F interface can have a finite SDIPS. However, the exact values of G_ϕ^F and G_ϕ^S are difficult to predict because they depend on the detailed microscopic structure of the interface. One possible approach is to consider G_ϕ^F and G_ϕ^S as fitting parameters which have to be determined from proximity-effect measurements. Note that the derivation of the boundary conditions (5) and (6) assumes a weak transmission probability per channel (tunnel limit), which seems reasonable considering the band-structure mismatch between most S and F materials. It furthermore assumes that the system is weakly polarized. However, there is no fundamental constraint on the amplitudes of G_T , G_ϕ^F , and G_ϕ^S because these parameters consist of a sum of contributions from numerous conducting channels.

In S/F circuits, long-range triplet correlations (between equal spins) can occur when the circuit includes several F electrodes or domains with noncolinear magnetizations.²¹ Recently, it has been found that this effect can also arise in S/F circuits with spin-active interfaces due to spin-flip interfacial coupling terms which are due, e.g., to some misaligned local moments at the S/F interface.²² In our work, we consider interfaces which are ‘‘spin active’’ in the sense that the SDIPS is finite. However, we assume that there is no interfacial spin-flip coupling and that F is uniformly polarized. Hence, we do not obtain any long-range triplet component with our model. Note that we also disregard spin-flip and spin-orbit scattering occurring inside the S and F layers (see, for instance, Refs. 23 and 24).

III. NUMERICAL TREATMENT OF THE PROBLEM

Equations (1)–(6) have already been solved numerically with a self-consistent procedure in the case $\gamma_\phi^S = \gamma_\phi^F = 0$ (see, e.g., Ref. 24). In this paper, we study the cases of finite γ_ϕ^S and γ_ϕ^F using a numerical treatment based on a relaxation method. This treatment is divided into two steps. We first calculate the values of $\Delta(x)$ and $\theta_{n,\sigma}$ self-consistently with a relaxation method in imaginary times. Then, we determine the pairing angle $\theta_\sigma(\varepsilon, x)$ corresponding to the calculated $\Delta(x)$ by using a similar relaxation method in real times, i.e., we use $\omega_n = -i\varepsilon + \Gamma$ and $\text{sgn}(\omega_n) = 1$ in Eqs. (1)–(6), with as ε the energy and $\Gamma = 0.05\Delta_0$ as a rate which accounts for inelastic processes.²⁵ Finally we obtain the DOS $N(\varepsilon, x) = \sum_\sigma N_\sigma(\varepsilon, x)$ at position x by using $N_\sigma(\varepsilon, x) = (N_0/2) \text{Re}\{\cos[\theta_\sigma(\varepsilon, x)]\}$, with $N_0/2$ as the normal DOS per spin direction. Throughout this numerical treatment, we use a discretized space, with a step of $0.001\xi_{S(F)}$ in $S(F)$. In the following, we mainly focus on $N_F(\varepsilon) = N(\varepsilon, x=d_F^-)$. Reference 17 studied analytically S/F bilayers with $d_S \leq \xi_S/2$, $\gamma_\phi^S \ll 1$, $\gamma_T \ll 1$, and $d_F \geq \xi_F$. Our approach allows one to go

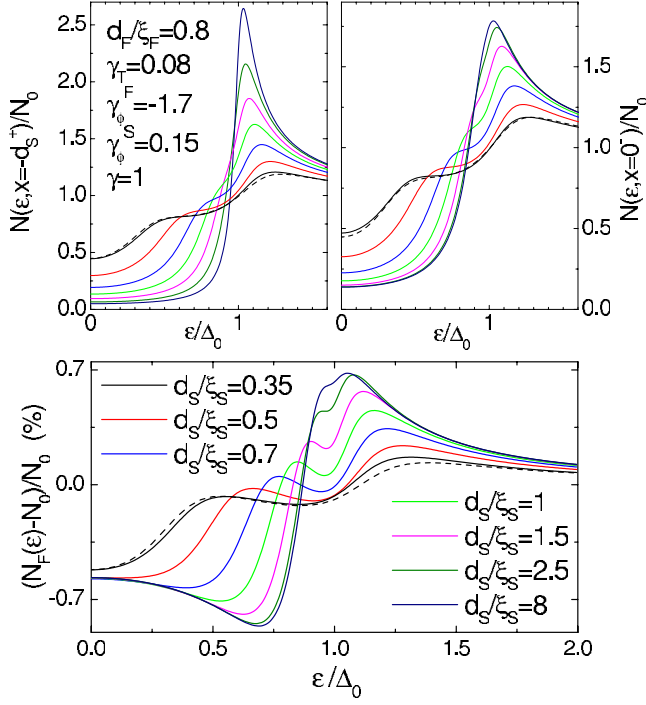


FIG. 1. (Color online) Densities of states $N(\epsilon, x=-d_S^+)$ (top left panel) and $N(\epsilon, x=0^-)$ (top right panel) at the left and right sides of the superconductor, respectively, and density of states $N_F(\epsilon)$ at the right side of the ferromagnet (bottom panel) plotted vs ϵ for different values of d_S . The full lines correspond to our numerical results. The black dashed lines correspond to the analytical predictions of Ref. 17 for $d_S/\xi_S=0.35$.

beyond this regime. Note that in Figs. 1–5, the results are shown for $E_{ex}=100\Delta_0$, $\Omega_D=601k_B T$, and $k_B T=0.1\Delta_0$.

IV. SDIPS-INDUCED DOUBLE GAP STRUCTURE

A. Variations of the bilayer spectrum with the thickness of S

The left and right top panels of Fig. 1 show the densities of states $N(\epsilon, x=-d_S^+)$ and $N(\epsilon, x=0^-)$ at the left and right

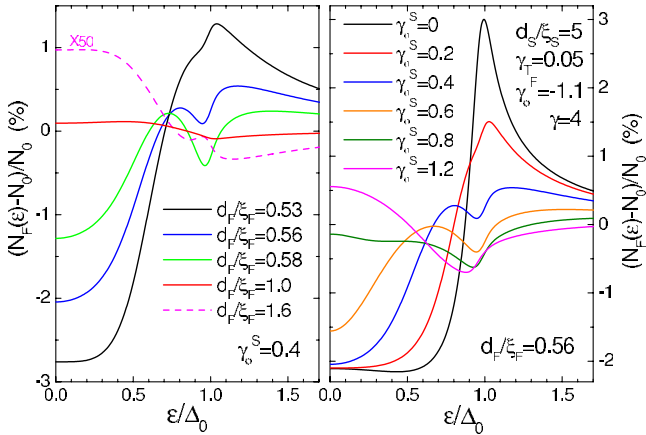


FIG. 2. (Color online) Density of states $N_F(\epsilon)$ at the right side of the ferromagnet plotted vs ϵ for different values of d_F (left panel) and different values of γ_ϕ^S (right panel). In the left panel, for $d_F/\xi_F=1.6$, we have multiplied $[N_F(\epsilon)-N_0]/N_0$ by a factor of 50 for visibility of the curve.

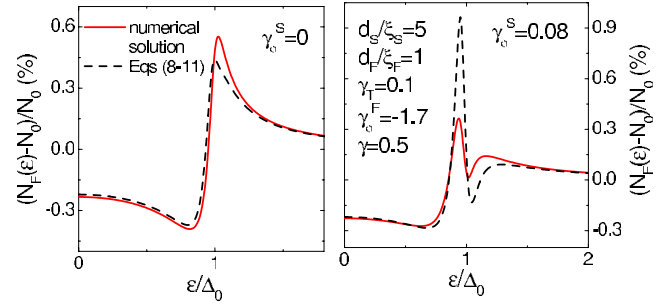


FIG. 3. (Color online) Density of states $N_F(\epsilon)$ at the right side of the ferromagnet plotted vs ϵ for $\gamma_\phi^S=0$ (left panel) and γ_ϕ^S finite (right panel). The solid lines are calculated from Eqs. (8)–(11) and the black dotted lines correspond to the self-consistent numerical resolution of Eqs. (1)–(6).

sides of the superconductor, respectively, for different values of d_S and the bottom panel of Fig. 1 shows the corresponding DOS $N_F(\epsilon)$ at the right side of F . For $d_S=0.35\xi_S$, the curves calculated with our numerical code (black full lines) are in close agreement with the analytical solution given in Ref. 17 (black dashed lines). The DOS is similar at the two sides of S and displays a DGS which reveals the existence of an effective Zeeman splitting of the form

$$\Delta_Z^{\text{eff}} = 2\Delta_0 \frac{\xi_S}{d_S} \gamma_\phi^S = E_{\text{Th}}^S \frac{G_S^S}{G_S} \quad (7)$$

with $E_{\text{Th}}^S = \hbar D_S/d_S^2$ as the Thouless energy of the S layer and $G_S = \sigma_S A/d_S$ as its normal-state conductance. The DGS is also visible in $N_F(\epsilon)$ due to the proximity effect. It becomes narrower when d_S increases, in agreement with Eq. (7), which indicates that Δ_Z^{eff} scales with d_S^{-1} . For very large values of d_S , the DOS $N(\epsilon, x=-d_S^+)$ at the left side of S tends to the bulk value $\text{Re}\{\cos[\theta_0(\epsilon)]\}$, with $\theta_0(\epsilon) = \arctan[\Delta_0/(-i\epsilon + \Gamma)]$. However, a DGS remains clearly visible in $N_F(\epsilon)$, a result which is quite counterintuitive considering the low- d_S expression Eq. (7) (see bottom panel, full line). Note that in the S layer, with the parameters of Fig. 1, $d_S \gg \xi_S$ and $\epsilon=0$ [$\epsilon=\Delta_0$], $N(\epsilon, x)$ decays from its bulk value to $N(\epsilon, x=0^-)$ in a distance on the order of ξ_S [$2\xi_S$] near the interface (not shown). In the large- d_S limit, the DOS $N(\epsilon, x=0^-)$ at the left side of the S/F interface does not show a clear DGS for the

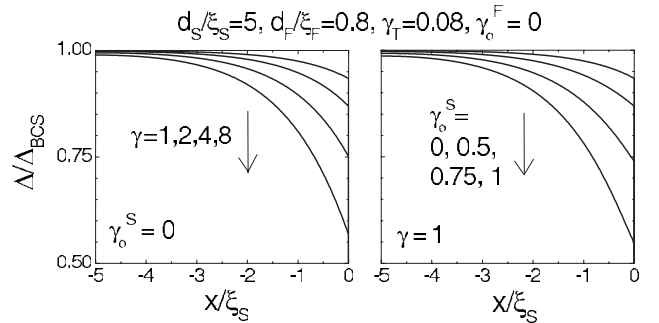


FIG. 4. Self-consistent superconducting gap $\Delta(x)$ vs the spatial coordinate x for different values of γ (left panel) and γ_ϕ^S (right panel).

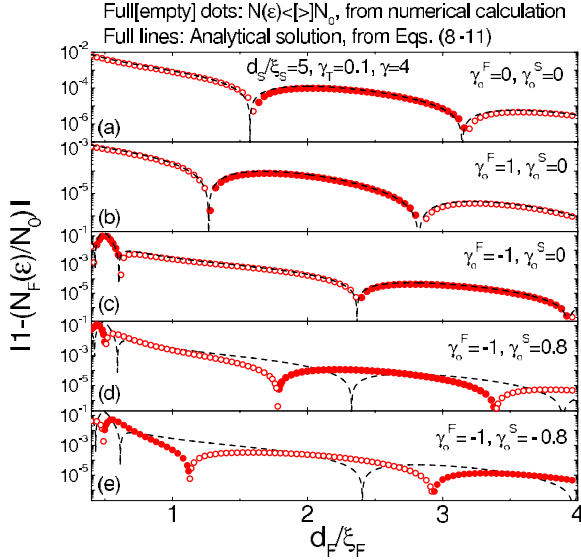


FIG. 5. (Color online) Zero-energy density of states $N_F(\varepsilon=0)$ at the right side of F versus the thickness d_F of F . The density of states calculated numerically is shown with dots. The full and empty dots correspond to $N_F(\varepsilon=0) < 0$ and $N_F(\varepsilon=0) > 0$, respectively. The density of states given by Eqs. (8)–(11) is shown with black dashed lines. Panel (a) corresponds to a case with no SDIPS ($\gamma_\phi^F = \gamma_\phi^S = 0$). Panels (b) and (c) show the effect of a finite γ_ϕ^F . Panels (d) and (e) show the effect of a finite γ_ϕ^S , in comparison with panel (c) where $\gamma_\phi^S = 0$. With the parameters used here, Eqs. (8)–(11) are in agreement with our numerical code only when $\gamma_\phi^S = 0$.

weak value of γ_ϕ^S used in Fig. 1 because of the strong DOS peak at $\varepsilon = \Delta_0$. However, a DGS would appear more clearly in $N(\varepsilon, x=0^-)$ for larger values of γ_ϕ^S , e.g., using $\gamma_\phi^S = 0.4$ (not shown). The DGS thus seems to persist at large values of d_S due to an effect which involves a S area with thickness $\sim \xi_S$ near the S/F interface and the whole F .

B. Variations of the bilayer spectrum with the thickness of F

Due to the ferromagnetic exchange field E_{ex} , the zero-energy DOS $N_F(\varepsilon=0)$ oscillates around its normal-state value N_0 when d_F increases.^{6,26–28} In the large- d_S limit, we find that the DGS can occur at the F side for both an ordinary [$N_F(\varepsilon=0) > N_0$] and a reversed [$N_F(\varepsilon=0) < N_0$] DOS. However, its visibility varies with d_F like in the limit $d_S \leq \xi_S/2$ of Ref. 17. Figure 2, left panel, shows N_F versus ε for different values of d_F and $d_S/\xi_S = 5$. From $d_F = 0.53\xi_F$ to $0.58\xi_F$, $N_F(\varepsilon=0) - N_0$ is positive and the visibility of the DGS increases (see black, blue, and green full lines). For $d_F = \xi_F$, $N_F(\varepsilon=0) - N_0$ is negative and the DGS is not visible anymore (see red full line). For $d_F = 1.6\xi_F$, the DGS is visible again, with both the inner and outer peaks of the DOS inverted due to $N_F(\varepsilon=0) - N_0 < 0$ (see dashed line).

C. Variations of the bilayer spectrum with G_ϕ^S

In the parameters range investigated by us (with in particular $E_{\text{ex}} \geq \Delta$, $0.35 \leq d_S/\xi_S \leq 10$, and $0.4 \leq d_F/\xi_F \leq 4$), no DGS occurs when $\gamma_\phi^S = 0$. The DGS studied in this paper thus seems to be a direct consequence of $\gamma_\phi^S \neq 0$ for large d_S/ξ_S as

well as small d_S/ξ_S . Figure 2, right panel, shows the variations of $N_F(\varepsilon)$ with γ_ϕ^S for a constant value of d_F . For $\gamma_\phi^S = 0$, no DGS appears. For a very small γ_ϕ^S (see full line, corresponding to $\gamma_\phi^S = 0.2$ or $G_\phi^S = G_T$), $N_F(\varepsilon)$ shows a change in slope which corresponds to a smoothed DGS, near $\varepsilon = \Delta_0$ (from Sec. IV B, this DGS occurs only for certain values of d_F). When γ_ϕ^S becomes sufficiently large, $N_F(\varepsilon)$ shows a clear DGS, i.e., two peaks, one above and one below $\varepsilon = \Delta_0$, while a local minimum is visible for $\varepsilon \sim \Delta_0$. The distance between the two peaks of $N_F(\varepsilon)$ increases with γ_ϕ^S . In Fig. 2, when γ_ϕ^S becomes too large ($\gamma_\phi^S \geq 0.8$), the sign of $N_F(\varepsilon = 0) - N_0$ changes. This suggests that γ_ϕ^S does not only induce DGSs but also shifts the oscillations of $N_F(\varepsilon)$ with d_F . This last effect will be investigated in more details for $\varepsilon = 0$ in Sec. V. With the parameters of Fig. 2, the DGS is not visible anymore when γ_ϕ^S becomes larger than approximately 1. In the general case, this threshold strongly depends on the different parameters characterizing the S/F bilayer.

D. Analytical description of the thick superconductor limit

In order to have a better insight on the persistence of the SDIPS-induced DGS at large values of d_S , we provide in this section an analytical description of the case where S is semi-infinite. For simplicity, we assume that the superconducting gap is only weakly affected by the presence of the F layer, i.e., $\Delta(x) = \Delta_0$. We furthermore assume that the proximity effect is weak, i.e., $\theta_{n,\sigma}(x \in F) \ll 1$ and $\theta_{n,\sigma}(x \in S) - \theta_n^0 \ll 1$, with $\theta_n^0 = \arctan(\Delta_0/|\omega_n|)$. In this case, the Usadel equations (1) and (2) lead to

$$\theta_{n,\sigma}(x) = \theta_{n,\sigma}^F \cosh\left[\frac{(x-d_F)k_{n,\sigma}}{\xi_F}\right] / \cosh\left(\frac{d_F k_{n,\sigma}}{\xi_F}\right) \quad (8)$$

for $x \in F$ and

$$\theta_{n,\sigma}(x) = \theta_n^0 + \delta\theta_{n,\sigma}^S \exp\left(\frac{x\eta_n}{\xi_S}\right) \quad (9)$$

for $x \in S$, with $\eta_n = [1 + (\omega_n/\Delta_0)^2]^{1/4}$. We have introduced in the above equations $\delta\theta_{n,\sigma}^S = \theta_{n,\sigma}(x=0^-) - \theta_n^0$ and $\theta_{n,\sigma}^F = \theta_{n,\sigma}(x=0^+)$. The linearization of the boundary conditions (5) and (6) with respect to these two quantities leads to

$$\theta_{n,\sigma}^F = \frac{\gamma_T [\sin(\theta_n^0) + \cos(\theta_n^0) \delta\theta_\sigma^S]}{\gamma_T \cos(\theta_n^0) + i\gamma_\phi^F \sigma \text{sgn}(\omega_n) + B_{n,\sigma}} \quad (10)$$

and

$$\delta\theta_{n,\sigma}^S = - \frac{\gamma\gamma_T + i\gamma_\phi^S \sigma \text{sgn}(\omega_n)}{\eta_n^3 + [\gamma\gamma_T + i\gamma_\phi^S \sigma \text{sgn}(\omega_n)] \frac{|\omega_n|}{\Delta_0}} \quad (11)$$

with $B_{n,\sigma} = k_{n,\sigma} \tanh[d_F k_{n,\sigma}/\xi_F]$. Importantly, Eqs. (8)–(11) are valid provided $\delta\theta_{n,\sigma}^S \ll 1$ and $\theta_{n,\sigma}^F \ll 1$, which requires $\gamma_T \ll 1$, $\gamma_\phi^S \ll 1$, and $d_F \geq \xi_F$. We have used these hypotheses to simplify Eq. (11). The validity of the approximation $\Delta(x) = \Delta_0$ will be discussed in Sec. V.

Figure 3 shows $N_F(\varepsilon)$ calculated from the analytical continuation of Eqs. (8)–(11) (black dashed lines) and from our numerical code (red full lines) for a weak value of γ and

$\gamma_\phi^S=0$ (left panel) or $\gamma_\phi^S \neq 0$ (right panel). The two calculations are in relatively good agreement.²⁹ For the parameters used in Fig. 3, we have checked numerically that the approximation $\Delta(x)=\Delta_0$ gives results in very good agreement with the full resolution of Eqs. (1)–(6). At $\varepsilon \sim \Delta_0$, small discrepancies arise between the predictions of the numerical code and of Eqs. (8)–(11) due to resonance effects which make $\delta\theta_{n,\sigma}^S$ and $\theta_{n,\sigma}^F$ larger than for $\varepsilon=0$ or $\varepsilon \gg \Delta_0$. Equations (8)–(11) allow one to recover the fact that a DGS can appear in $N_F(\varepsilon)$ due to $\gamma_\phi^S \neq 0$ (right panel). In the limit $d_S \gg \xi_S$, the pairing angle of the system cannot be put under the form $\theta_{\sigma}(x, \varepsilon) = \theta(x, \varepsilon - (\sigma\Delta_Z^{\text{eff}}/2))$, contrarily to what has been found for $d_S \leq \xi_S/2$. Therefore, the notion of SDIPS-induced effective Zeeman splitting is not valid for thick S layers. Nevertheless, from Eqs. (9) and (11), near the S/F interface, the resonance energies of the S spectrum can be spin dependent because quantum interferences make the superconducting correlations sensitive to the SDIPS on a distance on the order of ξ_S/η_n near the S/F interface. From Eqs. (8) and (10), this behavior is transmitted to the whole F layer due to the proximity effect. From Eq. (11), the energy scale related to the occurrence of the DGS has the form

$$\Delta_{\text{SDIPS}} = 2\Delta_0 \frac{G_\phi^S}{G_S} \quad (12)$$

with $\widetilde{G}_S = \sigma_S A / \xi_S$ as the normal-state conductance of a slab of thickness ξ_S of the S material. Interestingly, this expression has a form similar to Eq. (7), with d_S replaced with ξ_S (one has $2\Delta_0 = \hbar D_S / \xi_S^2 = \widetilde{E}_{\text{Th}}^S$). Note that for a ballistic S/F single-channel contact, the SDIPS also produces a spin-dependent resonance effect.³⁰ However, in this case, one does not obtain a DGS but rather a subgap resonance in the conductance and the zero-frequency noise of the system.

V. SELF-CONSISTENT SUPERCONDUCTING GAP AND ZERO-ENERGY DOS OF F

For completeness, we now discuss the effects of the SDIPS on the self-consistent superconducting gap $\Delta(x)$ and the zero-energy DOS $N_F(\varepsilon=0)$ versus d_F . It is already known that the amplitude of $\Delta(x)$ decreases when γ_T or γ increases, similarly to what happens in a S /normal-metal bilayer.³¹ Figure 4 compares the effects of γ (left panel) and γ_ϕ^S (right panel) on $\Delta(x)$ (it only shows the effect of $\gamma_\phi^S > 0$, but the effect of $\gamma_\phi^S < 0$ is similar). One can see that $\Delta(x)$ significantly decreases when $|\gamma_\phi^S|$ increases. Similarly, in a clean superconductor connected to a ferromagnetic insulator (FI), $\Delta(x)$ has been predicted to decrease due to the spin dependence of the reflection phases against FI.³² In contrast, in the regime of parameters investigated by us, γ_ϕ^F has a negligible effect on the value of $\Delta(x)$ because it does not occur directly in boundary condition (11) at the S side of the interface. From this brief study of $\Delta(x)$, we conclude that the approximation $\Delta(x)=\Delta_0$ used in Sec. IV D is valid only for sufficiently small values of γ_T , γ , and γ_ϕ^S .

Figure 5 presents the effects of γ_ϕ^F and γ_ϕ^S on the variations of $N_F(\varepsilon=0)$ with d_F . The DOS calculated numerically is shown with symbols and the DOS given by Eqs. (8)–(11)

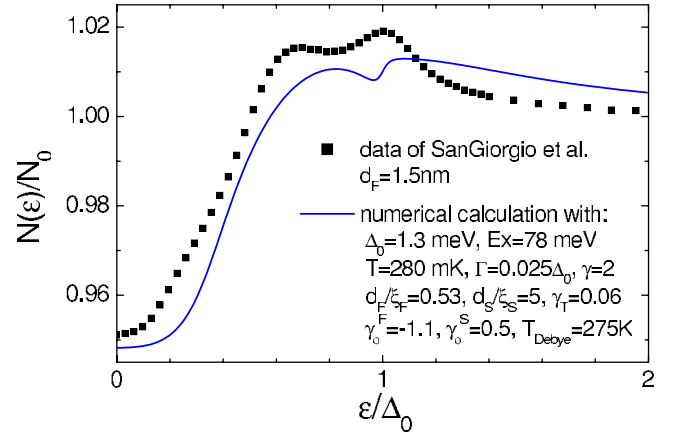


FIG. 6. (Color online) Comparison between the data of SanGiorgio *et al.* (Ref. 10) for $d_S=1.5$ nm and our numerical calculation with $\Delta_0=1.3$ meV, $E_{\text{ex}}=78$ meV, $k_B T=280$ mK, $d_F/\xi_F=0.53$, $d_S/\xi_S=5$, $\gamma_T=0.06$, $\gamma_\phi^F=-1.1$, $\gamma_\phi^S=0.5$, $\gamma=2$, $T_D=275$ K, and $\Gamma=0.025\Delta_0$.

is shown with full lines. In panels (a)–(c), we have used $\gamma_\phi^S=0$, so that the two calculations are in close agreement. In panels (d) and (e), the two calculations strongly differ because γ_ϕ^S is too large for the hypotheses leading to Eqs. (8)–(11) to be valid. We recover the fact that, in the regime $d_F \geq \xi_F$, $N_F(\varepsilon=0)$ shows exponentially damped oscillations with d_F .^{6,26} In the regime $d_F \leq \xi_F$, the oscillations of $N_F(\varepsilon=0)$ with d_F are less regular. This can be understood from the analytical description of Sec. IV D. For $d_F \geq \xi_F$, one has $B_{n,\sigma} \sim k_{n,\sigma}$, so that $N_F(\varepsilon=0)$ depends on d_F through the $\cosh(d_F k_{n,\sigma} / \xi_F)$ term of Eq. (8) only. For $d_F \leq \xi_F$, $B_{n,\sigma}$ and thus $\theta_{n,\sigma}^F$ strongly depend on d_F , which complicates the variations of $N_F(\varepsilon=0)$ with d_F and leads to more irregular oscillations. Reference 13 already showed that γ_ϕ^F can shift the oscillations of $N_F(\varepsilon=0)$ with d_F . Panels (b) and (c) confirm this result and also show that a positive (negative) γ_ϕ^F decreases (increases) the amplitude of $N_F(\varepsilon=0)$. From panels (d) and (e), γ_ϕ^S can also significantly shift the oscillations of $N_F(\varepsilon=0)$ with d_F , in agreement with Fig. 2, right panel. For the parameters used in Fig. 5, γ_ϕ^S does not modify spectacularly the amplitude of $N_F(\varepsilon)$. For larger values of $|\gamma_\phi^S|$, the amplitude of the superconducting proximity effect would significantly decrease due to a reduction in $\Delta(x)$ (not shown).

VI. DISCUSSION ON THE DATA OF REFERENCE 10

We now consider the DOS measurements realized by SanGiorgio *et al.*¹⁰ for Nb/Ni bilayers with $d_S=50$ nm. From Ref. 18 which considers samples fabricated by the same team, one has $\xi_S \sim 10$ nm, so that $d_S/\xi_S \sim 5$. However, double gap structures have been observed by SanGiorgio *et al.*, which motivates a comparison with our model.

Figure 6 compares the data measured for $d_F=1.5$ nm (black squares) with our numerical calculation (full line). Our calculation reproduces almost quantitatively the experimental curve. We have used $d_F=1.5$ nm, $d_S/\xi_S=5$, and $T=280$ mK, in agreement with Refs. 10 and 18. We have also used the exchange field $E_{\text{ex}}=78$ meV, estimated by Ref. 10,

and the Debye temperature $T_D=275$ K of Nb, taken from Ref. 33. We have assumed $\xi_F=2.83$ nm, $\gamma_T=0.06$, $\gamma_\phi^F=-1.1$, $\gamma_\phi^S=0.5$, and $\Gamma=0.025\Delta_0$. Note that from Ref. 18, one has $\sigma_S^{-1}\sim 15.9$ $\mu\Omega$ cm and $\sigma_F^{-1}\sim 9.7$ $\mu\Omega$ cm, so that one should have $\gamma=\xi_S\sigma_F/\xi_F\sigma_S\sim 2.9$ with the above values of ξ_S and ξ_F . In Fig. 6, we have used a value $\gamma=2$, which is in relatively good agreement with this estimate. The values of γ_T , γ_ϕ^F , γ_ϕ^S , and γ used in the fit yield $G_\phi^F/G_T\sim 18$ and $G_\phi^S/G_T\sim 4$. A theoretical prediction of these ratios is very difficult because they depend on the detailed microscopic structure of the Nb/Ni interface. However, with a simple delta function barrier model, it is already possible to find situations where G_ϕ^S and G_ϕ^F are larger than G_T (see Appendix A and Fig. 6 of Ref. 17). Therefore, we think that the SDIPS parameters used by us are possible.

We cannot reproduce quantitatively the data obtained by SanGiorgio *et al.* for all values of d_F with the same set of parameters as for $d_F=1.5$ nm. We think that this might be due to the fact that some characteristics of the samples such as, e.g., E_{ex} and thus ξ_F , γ_ϕ^F , γ_ϕ^S , and γ can vary with d_F .³⁴ In the data of SanGiorgio *et al.*, from $d_F=1.5$ nm to $d_F=3.0$ nm, the distance between the two peaks of the DGS increases like in our model (see Fig. 2, left panel). However, the outer peak of the DGS remains very close to $\varepsilon\sim\Delta_0$, which seems difficult to reproduce with our model. Note that in Ref. 10, for $d_F=3.5$ nm, the outer peaks of the DOS are inverted, whereas a sharp dip occurs at low energies, which can give the impression that the inner peaks of the DOS persist but are not inverted, in contrast to what we find (see Sec. IV B). However, we think that the observation of this zero-bias dip is not totally reliable. Indeed, SanGiorgio *et al.* explained that, in the DOS of their thickest samples (for $d_F>3.5$ nm), “the zero-bias peak is due to the steep voltage dependence of the background conductance and is therefore a by-product of the data normalization procedure.” The zero-bias dip of the $d_F=3.5$ nm sample occurs on the same energy scale as these zero-bias peaks, and it goes together with a strange zero-bias singularity similar to those shown by the thickest samples. Therefore, we are not sure whether a

proper interpretation of the data of Ref. 10 must take into account this feature. Reference 35 suggests that the DGS observed by SanGiorgio *et al.* could be due to triplet correlations. However, it is difficult to know whether this interpretation can be more satisfying than ours because Ref. 35 does not show any quantitative interpretation of the data and does not discuss, for instance, the evolution of the inner and outer peak positions with d_F .

VII. CONCLUSION

In summary, we have calculated the density of states (DOS) in a diffusive *S/F* bilayer with a spin-active interface. We have used a self-consistent numerical treatment to make a systematic study of the effects of the SDIPS. We characterize the SDIPS with two conductance-like parameters G_ϕ^S and G_ϕ^F , which occur in the boundary conditions describing the *S* and *F* sides of the interface, respectively. We find that the amplitude of $\Delta(x)$ significantly decreases if G_ϕ^S is too strong, whereas it is almost insensitive to G_ϕ^F . In contrast, both G_ϕ^S and G_ϕ^F can shift the oscillations of the zero-energy DOS of *F* with the thickness of *F*. Remarkably, we find that the SDIPS can produce a double gap structure in the DOS of *F*, even when the *S* layer is much thicker than the superconducting coherence length. This leads to DOS curves which have striking similarities with those of Ref. 13. More generally, our results could be useful for interpreting future experiments on superconducting/ferromagnetic diffusive hybrid structures.

ACKNOWLEDGMENTS

We acknowledge interesting discussions with A. A. Golubov, T. Kontos, M. Yu. Kupriyanov, and N. Regnault. We thank P. SanGiorgio and M. Beasley for discussions and for sending us their data. J.L. was supported by the Research Council of Norway under Grants No.158518/431, No. 158547/431 (NANOMAT), and No. 167498/V30 (STOR-FORSK).

¹A. A. Golubov, M. Yu. Kupriyanov, and E. Il'ichev, Rev. Mod. Phys. **76**, 411 (2004).
²A. I. Buzdin, Rev. Mod. Phys. **77**, 935 (2005).
³W. Guichard, M. Aprili, O. Bourgeois, T. Kontos, J. Lesueur, and P. Gandit, Phys. Rev. Lett. **90**, 167001 (2003).
⁴L. B. Ioffe, V. B. Geshkenbein, M. V. Feigel'man, A. L. Fauchère, and G. Blatter, Nature (London) **398**, 679 (1999).
⁵T. Yamashita, K. Tanikawa, S. Takahashi, and S. Maekawa, Phys. Rev. Lett. **95**, 097001 (2005).
⁶T. Kontos, M. Aprili, J. Lesueur, and X. Grison, Phys. Rev. Lett. **86**, 304 (2001).
⁷T. Kontos, M. Aprili, J. Lesueur, X. Grison, and L. Dumoulin, Phys. Rev. Lett. **93**, 137001 (2004).
⁸L. Crétonin, A. K. Gupta, H. Sellier, F. Lefloch, M. Fauré, A. Buzdin, and H. Courtois, Phys. Rev. B **72**, 024511 (2005).
⁹S. Reymond, P. SanGiorgio, M. R. Beasley, J. Kim, T. Kim, and

K. Char, Phys. Rev. B **73**, 054505 (2006).

¹⁰P. SanGiorgio, S. Reymond, M. R. Beasley, J. H. Kwon, and K. Char, Phys. Rev. Lett. **100**, 237002 (2008).

¹¹M. Yu. Kupriyanov and V. F. Lukichev, Sov. Phys. JETP **67**, 1163 (1988).

¹²D. Huertas-Hernando, Y. V. Nazarov, and W. Belzig, arXiv:cond-mat/0204116 (unpublished); D. Huertas-Hernando, Ph.D. thesis, Delft University of Technology, The Netherlands, 2002; D. Huertas-Hernando, Y. V. Nazarov, and W. Belzig, Phys. Rev. Lett. **88**, 047003 (2002).

¹³A. Cottet and W. Belzig, Phys. Rev. B **72**, 180503(R) (2005).

¹⁴The SDIPS is called by some other authors “spin-mixing angle” or “spin-rotation angle.” However, in our case, we consider a single ferromagnet which is uniformly polarized, so that the notions of mixing or rotation are not relevant.

- ¹⁵The effects of the SDIPS on S/F systems have been initially studied in the ballistic case (see, e.g., Refs. [16](#) and [32](#)).
- ¹⁶A. Millis, D. Rainer, and J. A. Sauls, *Phys. Rev. B* **38**, 4504 (1988).
- ¹⁷A. Cottet, *Phys. Rev. B* **76**, 224505 (2007).
- ¹⁸J. Kim, J. H. Kwon, K. Char, H. Doh, and H.-Y. Choi, *Phys. Rev. B* **72**, 014518 (2005).
- ¹⁹Th. Mühge, K. Westerholt, H. Zabel, N. N. Garif'yanov, Yu. V. Goryunov, I. A. Garifullin, and G. G. Khaliullin, *Phys. Rev. B* **55**, 8945 (1997).
- ²⁰N. B. Kopnin, *Theory of Nonequilibrium Superconductivity* (Clarendon, Oxford, 2001); W. Belzig, F. K. Wilhelm, C. Bruder, G. Schön, and A. D. Zaikin, *Superlattices Microstruct.* **25**, 1251 (1999).
- ²¹F. S. Bergeret, A. F. Volkov, and K. B. Efetov, *Rev. Mod. Phys.* **77**, 1321 (2005).
- ²²M. Eschrig, J. Kopu, J. C. Cuevas, and Gerd Schön, *Phys. Rev. Lett.* **90**, 137003 (2003); Y. Asano, Y. Sawa, Y. Tanaka, and A. A. Golubov, *Phys. Rev. B* **76**, 224525 (2007); A. V. Galaktionov, M. S. Kalenkov, and A. D. Zaikin, *ibid.* **77**, 094520 (2008); M. Eschrig and T. Lofwander, *Nat. Phys.* **4**, 138 (2008).
- ²³E. A. Demler, G. B. Arnold, and M. R. Beasley, *Phys. Rev. B* **55**, 15174 (1997); S. Oh, Y.-H. Kim, D. Youm, and M. R. Beasley, *ibid.* **63**, 052501 (2000); L. Crépinon, A. K. Gupta, H. Sellier, F. Lefloch, M. Fauré, A. Buzdin, and H. Courtois, *ibid.* **72**, 024511 (2005); M. Fauré, A. I. Buzdin, A. A. Golubov, and M. Yu. Kupriyanov, *ibid.* **73**, 064505 (2006); F. S. Bergeret, A. F. Volkov, and K. B. Efetov, *ibid.* **75**, 184510 (2007); J. Linder, T. Yokoyama, and A. Sudbo, *ibid.* **77**, 174514 (2008).
- ²⁴D. Yu. Gusakova, A. A. Golubov, M. Yu. Kupriyanov, and A. Buzdin, *JETP Lett.* **83**, 327 (2006).
- ²⁵W. Belzig, Ph.D. thesis, Karlsruhe University, 1999.
- ²⁶A. Buzdin, *Phys. Rev. B* **62**, 11377 (2000); I. Baladié and A. Buzdin, *ibid.* **64**, 224514 (2001).
- ²⁷M. Zareyan, W. Belzig, and Yu. V. Nazarov, *Phys. Rev. Lett.* **86**, 308 (2001); *Phys. Rev. B* **65**, 184505 (2002).
- ²⁸F. S. Bergeret, A. F. Volkov, and K. B. Efetov, *Phys. Rev. B* **65**, 134505 (2002).
- ²⁹For the parameters of Figs. [1](#) and [2](#), Eqs. [\(8\)](#)–[\(11\)](#) are not in good agreement with our numerical results because the hypotheses leading to these equations are not satisfied (see Sec. [V](#)).
- ³⁰A. Cottet and W. Belzig, *Phys. Rev. B* **77**, 064517 (2008).
- ³¹A. A. Golubov and M. Yu. Kupriyanov, *Sov. Phys. JETP* **69**, 805 (1990).
- ³²T. Tokuyasu, J. A. Sauls, and D. Rainer, *Phys. Rev. B* **38**, 8823 (1988).
- ³³N. W. Ashcroft and N. D. Mermin, *Solid State Physics* (Saunders College, Philadelphia, 1976).
- ³⁴T. Kontos, Ph.D. thesis, Université Paris-Sud, Orsay, France, 2002.
- ³⁵A. F. Volkov and K. B. Efetov, *Phys. Rev. B* **78**, 024519 (2008).